Breast Cancer
https://doi.org/10.1007/s12282-024-01549-7

SPECIAL FEATURE

Clinical application with deep learning

Deep learning model to predict Ki-67 expression of breast cancer using digital breast tomosynthesis

Ken Oba[1] · Maki Adachi[2] · Tomoya Kobayashi[2] · Eichi Takaya[3] · Daiki Shimokawa[2] · Toshinori Fukuda[4] · Kengo Takahashi[2] · Kazuyo Yagishita[1] · Takuya Ueda[2,3] · Hiroko Tsunoda[1]

Received: 9 October 2023 / Accepted: 24 January 2024

Abstract

Background Developing a deep learning (DL) model for digital breast tomosynthesis (DBT) images to predict Ki-67 expression.

Methods The institutional review board approved this retrospective study and waived the requirement for informed consent from the patients. Initially, 499 patients (mean age: 50.5 years, range: 29–90 years) referred to our hospital for breast cancer were participated, 126 patients with pathologically confirmed breast cancer were selected and their Ki-67 expression measured. The Xception architecture was used in the DL model to predict Ki-67 expression levels. The high Ki-67 vs low Ki-67 expression diagnostic performance of our DL model was assessed by accuracy, sensitivity, specificity, areas under the receiver operating characteristic curve (AUC), and by using sub-datasets divided by the radiological characteristics of breast cancer.

Results The average accuracy, sensitivity, specificity, and AUC were 0.912, 0.629, 0.985, and 0.883, respectively. The AUC of the four subgroups separated by radiological findings for the mass, calcification, distortion, and focal asymmetric density sub-datasets were 0.890, 0.750, 0.870, and 0.660, respectively.

Conclusions Our results suggest the potential application of our DL model to predict the expression of Ki-67 using DBT, which may be useful for preoperatively determining the treatment strategy for breast cancer.

Keywords DBT · FFDM · Ki-67 · Breast cancer · Deep learning

Introduction

Breast cancer is the most common cancer affecting women and its incidence and mortality rates are expected to increase [1]. Determining the molecular subtypes of breast cancer is crucial for its treatment [2]. Although the subtypes were originally classified based on gene expression, genetic testing is not clinically practical in all cases. Therefore, subtypes are often classified based on immunohistochemical assessment of biomarkers in clinical situations, including the estrogen receptor (ER), progesterone receptor, and human epidermal growth factor receptor 2 (HER2) [3]. However, surrogate subtypes do not always correspond to the molecular subtypes. Ki-67 is also a routinely used molecular biomarker, considered an independent prognostic factor for patients with breast cancer and expressed as the percentage of positively stained nuclei [4]. Ki-67 expression level is used as a reference for determining indications for chemotherapy, especially in ER-positive HER2-negative breast cancer [5, 6]. Ki-67 is typically assessed using needle biopsy specimens obtained via invasive procedures [4].

Several studies have tried to correlate the radiological findings associated with the expression of Ki-67 in breast

✉ Takuya Ueda
takuya.ueda.d3@tohoku.ac.jp

1 Department of Radiology, St. Luke's International Hospital, 9-1 Akashi-Cho, Chuo-Ku, Tokyo 104-8560, Japan

2 Department of Clinical Imaging, Tohoku University Graduate School of Medicine, 2-1 Seiryo-Machi, Aoba-Ku, Sendai, Miyagi 980-8575, Japan

3 AI Lab, Tohoku University Hospital, 1-1 Seiryo-Machi, Aoba-Ku, Sendai, Miyagi 980-8574, Japan

4 Department of Radiology, Oregon Health of Science University, 3181 SW Sam Jackson Park Rd, Portland, OR 97239-2098, USA

Published online: 07 March 2024

cancer [7–10], and many have reported the application of radiomics analysis to predict Ki-67 expression from radiological images [10–12]. Currently, the emphasis is on the potential usefulness of applying deep learning (DL) models, especially convolutional neural networks (CNN), for clinical imaging, such as the benign and malignant classification of breast lesions using MRI [13].

Recently, digital breast tomosynthesis (DBT) has emerged as a critical tool in breast imaging and has been utilized for breast cancer screening and diagnosis [14]. DBT presents several advantages over other imaging modalities such as FFDM (full-field digital mammography), US, and MRI. FFDM remains the standard for initial screening, however, DBT allows for more detailed evaluations and provides a series of thin-sliced images. Compared to ultrasound, DBT requires less operator expertise, enhancing its utility as an initial radiological examination tool in breast cancer diagnostics. Dissimilar to MRI, DBT provides detailed breast images without requiring contrast agents. DBT is also valued for its cost-effectiveness compared to other imaging modalities, adding to its advantages, and making it a viable option in clinical practice.

This study aims to develop a DL model for DBT imaging to predict Ki-67 expression.

Materials and methods

The Institutional Review Board approved this retrospective study and waived the requirement for written informed consent.

Data collection

A total of 499 patients (mean age, 50.5 years, 29–90 years) who were referred to our hospital for breast cancer, admitted, and underwent DBT between March 1, 2019, and August 31, 2019, were initially enrolled in this study. We reviewed the clinical and pathological information of each patient using our electronic medical records system. The exclusion criteria were as follows: (a) patients who underwent only unilateral breast imaging, (b) male patients, (c) postoperative patients, (d) patients with metal clips after biopsy, and (e) patients whose lesions could not be detected by DBT (Fig. 1). Of the 425 patients, we selected 126 with pathologically confirmed breast cancer and measured their Ki-67 levels.

Pathological evaluation and measurement of Ki-67 index

Table 1 shows the tumor characteristics. The pathological results and Ki-67 proliferation index were determined using the results of the preoperative biopsy. The pathological

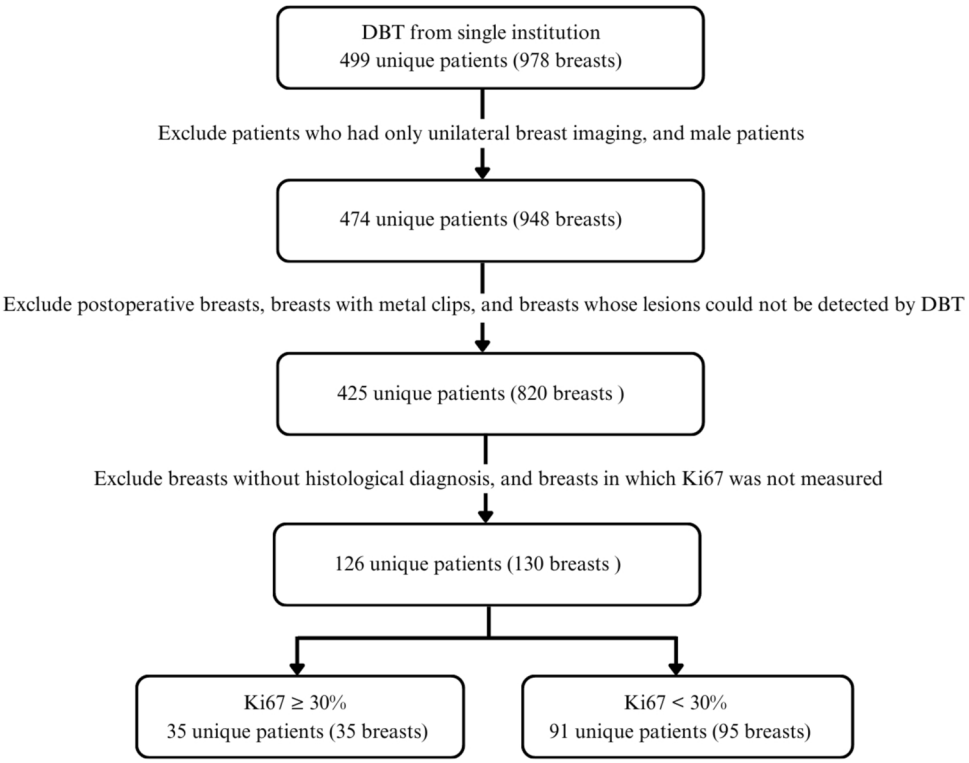

Fig. 1 Flowchart of inclusion and exclusion criteria. In total, 126 patients were included in this study. *DBT* digital breast tomosynthesis

Table 1 Patients and tumor characteristics

	High-Ki67	Low-i67
Ki-67 index Mean (%) ± SD (Min–Max)	48.42 ± 12.61 (31–74)	14.90 ± 7.80 (1–29)
Breasts (n)	35	95
Patients (n)	35	91
Histopathology*		
IDC, n (%)	30 (86)	70 (74)
Mucinous carcinoma, n (%)	1 (3)	4 (4)
Invasive micropapillary carcinoma, n (%)	0 (0)	1 (1)
ILC, n (%)	1 (3)	11 (12)
Microinvasive carcinoma, n (%)	1 (3)	1 (1)
DCIS, n (%)	2 (6)	8 (8)

High-Ki67 high Ki-67 lesion, *Low-Ki67* low Ki-67 lesion, *IDC* invasive ductal carcinoma, *ILC* invasive lobular carcinoma, *DCIS* ductal carcinoma in situ, *SD* standard deviation, *Min* minimum, *Max* maximum

*No significant difference

results of the 126 patients with breast cancer included invasive ductal carcinoma in 100 patients, mucinous carcinoma in five patients, invasive micropapillary carcinoma in one patient, invasive lobular carcinoma in 12 patients, microinvasive carcinoma in two patients, and ductal carcinoma in situ (DCIS) in 10 patients.

The Ki-67 proliferation index was evaluated by manual counting. Herein, we applied a 30% threshold for Ki-67 expression based on the recommendations of the St. Gallen 2021 Ki-67 Working Group statement [6]. Multiple studies have emphasized the challenges associated with the reproducibility of intermediate proliferation, particularly within the range of 15–30% [20]. To address this issue and ensure consistency, we chose a threshold of 30% to categorize Ki-67 expression, ensuring a more robust and standardized framework for the assessment of proliferative activity in breast cancer specimens. Each lesion was classified into two groups: high Ki-67 lesion (High-Ki67) that showed a Ki-67 proliferation index of >30% (35 lesions), and low Ki-67 lesion (Low-Ki67) that showed Ki-67 proliferation of <30% (95 lesions).

DBT examinations

All DBT images were acquired on 3Dimentions Mammography System (Hologic Inc., Bedford, MA, USA). Scanning parameters of DBT images are as follows: kilovoltage peak ranges of 25–34 kV; current ranges of 10–180 mA; exposed time ranges of 51–368 ms; force ranges of 48.9–142.7 N; thick ranges of 16–92 mm; and absorbed dose ranges of 6.10–4.70 mGy. The total tomographic angler range was 15° (-7.5°—7.5°), consisting of 15 projection views taken at 1° increments. Interslice interval was 1 mm, and resolution was 70 × 70 µm per pixel. This study used mediolateral oblique view images.

Two radiologists with 5 and 30 years of experience annotated the lesions and classified the radiological findings into four categories: calcification, mass, distortion, and focal asymmetric density (FAD). All breast lesions were cropped to the center and resized to a grayscale image of 256 × 256 pixels.

DBT image datasets for the DL model training and test

Based on the annotation process by the radiologists, 2,977 images from 126 patients were selected for analysis. The DBT image dataset was divided into training/validation and test datasets in an 8:2 ratio, resulting in 2,372 and 605 images, respectively. The DBT image dataset was randomly divided into two datasets: 80 and 20% for the training/validation and test datasets, respectively. We ensured no overlapping images from the same patient between the training/validation and test datasets.

DL model

Our DL model was constructed using the Xception architecture [21], with pretraining and initialization of the CNN architecture using ImageNet [22]. RAdam was used for optimization and binary cross-entropy was used as the loss function with 10,000 steps, a warm-up proportion of 0.1, and a minimum learning rate of 1e-5 [12, 23]. The batch size and the number of epochs were set to 200 and 400, respectively.

Our computing system consists of an Intel Core i7-7800X CPU with six cores (Intel, Santa Clara, CA, USA) and an NVIDIA Quadro RTX 8000 GPU with 48 GB of memory (Nvidia, Santa Clara, CA, USA). The operating system was Ubuntu 18.04.5 long-term support: Xenial Xerus. Python

3.8.2 and Keras 2.2.0 with TensorFlow 1.9.0 were used as the deep learning framework.

Statistical analysis

Student's t-test was used to analyze quantitative continuous variables of clinical factors, whereas the chi-square test was used for discrete variables. Statistical significance was set at $p < 0.05$.

The performance of our DL model was assessed on the test dataset for accuracy, sensitivity, specificity, and the area under the curve (AUC) of the receiver operating characteristic (ROC) curve. In this study, true-positive (TP) lesions were defined as the correct classification of High-Ki67, while true-negative (TN) lesions were defined as the correct classification of Low-Ki67. False positive (FP) lesions were defined as the incorrect classification of Low-Ki67 as High-Ki67 and false negative (FN) lesions were defined as the incorrect classification of High-Ki67 as Low-Ki67. The sensitivity and specificity values are for a 0.5 probability cut line. Each value is calculated as follows:

$$\text{Accuracy} = (TP + TN)/(TP + FP + FN + TN)$$

$$\text{Sensitivity} = TP/(TP + FN)$$

$$\text{Specificity} = TN/(TN + FP)$$

To evaluate the diagnostic accuracy of each radiological finding, the datasets were divided into four sub-datasets: calcification, mass, distortion, and FAD. The diagnostic accuracy of our DL model for each sub-dataset was independently evaluated to examine the relationship between high Ki-67 vs low Ki-67 expression diagnostic performance and radiological findings.

Results

The clinical characteristics of the patients included in this study are presented in Table 1. The mean age of the High-Ki67 and Low-Ki67 groups were 50.29 ± 10.53 (range 36–81) and 54.39 ± 12.96 (range 32–88) years, respectively. There was no significant difference in age between the two groups.

Figure 2 shows the ROC curve of the DL model. The AUC value for the DL model was 0.883. The accuracy, sensitivity, and specificity of the DL model were 0.912, 0629, and 0.985, respectively. Table 2 shows the diagnostic accuracy of the four subgroups separated by radiological findings: 0.890 for the mass sub-dataset, 0.750 for the calcification sub-dataset, 0.870 for the distortion sub-dataset, and 0.660 for the FAD sub-dataset. Figure 3 illustrates representative images of TP, TN, FP, and FN lesions.

Discussion

Our research indicates the potential clinical application of the DL model for predicting Ki-67 expression using breast cancer imaging before surgery. Because Ki-67 expression is an important indicator that also influences breast cancer subtype classification, the early prediction of Ki-67 expression through clinical images before obtaining biopsy results can have potential benefits by enabling early decision-making regarding the initial treatment strategy.

Previous studies have reported the usefulness of radiomics analysis for predicting Ki67 values in breast cancer [12, 23]. Despite the different cut-off values for positive Ki-67 status, our DL model showed higher AUC values than previous radiomic analyses [12, 23]. Previous studies have suggested that the results of radiomics analysis may vary significantly depending on the setting of the ROI owing to the tumor heterogeneity of breast cancer, such as the periphery or inside of the tumor [24], and the robustness of radiomics analysis is highly affected by this parameter [24]. The DL model using CNN to convolute the morphological information on images allows comprehensive information to be captured throughout the entire tumor. Therefore, the proposed DL model offers more consistent and reliable insights.

Although image-based prediction of Ki-67 expression has also been investigated using various imaging modalities, such as MRI [25], our DL model used DBT as the imaging modality. DBT, an advanced imaging modality for FFDM, has become a widely used and commonly employed breast-imaging technique. Our DL models using widely available DBT imaging have the potential advantage of clinical applications over MRI. In addition, as DBT provides more detailed morphological information of tumors than FFDM, it may accurately reflect tumor heterogeneity [26].

Our results suggest that the predictive accuracy of Ki-67 expression varies among the sub-datasets of the radiological characteristics of breast cancer. The accuracy in the mass sub-dataset was higher compared to the other sub-datasets, whereas that in the calcification sub-dataset was lower compared to the other sub-datasets. This pattern is consistent with previous research, where a lower accuracy of calcification compared to other findings was observed in predicting the presence of stromal invasion in breast cancer [22]. It was also suggested that the DL model did not represent the relationship between calcification and invasion because of down-sampling image processing for DBT images [22]. We assumed the same reason for the lower accuracy in predicting Ki-67 expression in the calcification sub-dataset. The accuracy in the distortion sub-dataset was lower than that in the mass sub-dataset and

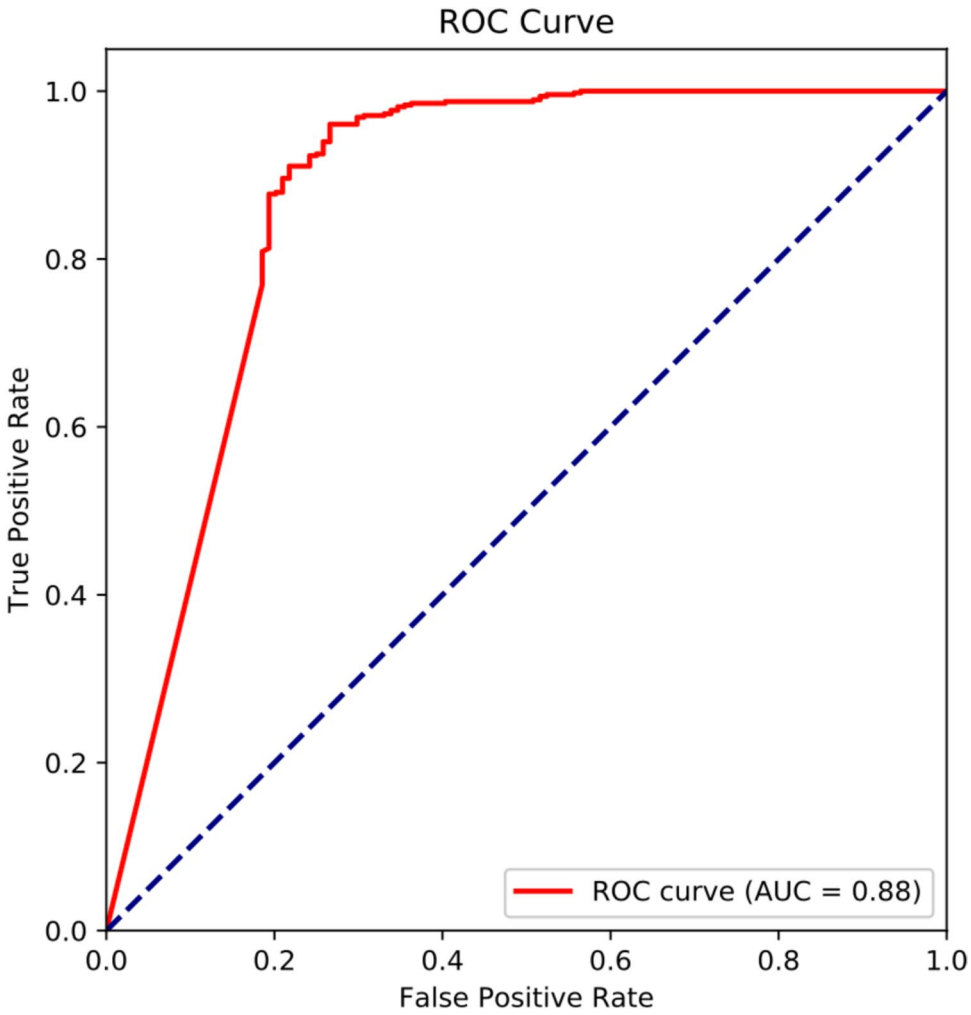

Fig. 2 Receiver operation characteristic curves. Receiver operating characteristic curves (ROC) for testing, based on the Ki-67 cut-off value of 30%. *AUC* area under the curve

Table 2 Diagnostic accuracy of four groups

	Accuracy	Sensitivity	Specificity
Mass	0.89	0.72	0.95
Calcification	0.75	0.64	0.82
Distortion	0.87	0.64	0.94
FAD	0.66	-	0.66

FAD focal asymmetric density

lower than that in the calcification sub-dataset. Although image interpretation is sometimes difficult, the presence of distortion is considered pathognomonic for malignancy when detected once. Therefore, it is reasonable that the accuracy of distortion would fall between that of the mass and calcification. The FAD sub-dataset did not show any clear trends, which may be associated with the small number of cases.

Ki-67 expression is a widely used biomarker in clinical practice and many thresholds have been applied across different contexts. For instance, in the classification of luminal subtypes of breast cancer, the 2011 St. Gallen Conference introduced a threshold of 14% [27], while the 2013 St. Gallen Conference raised it to 20% [28]. The monarchE trial, a randomized controlled study combining Abemaciclib with endocrine therapy, established an eligibility criterion of 20% or higher Ki-67 levels [28]. In the context of ER-positive HER2-negative breast cancer, both the 2022 breast cancer treatment guidelines and International Ki67 in Breast Cancer Working Group support a higher threshold of 30% or above [6, 29]. The challenge of reproducibility in measuring intermediate levels of proliferation activity, particularly within the range of 15–30%, has been highlighted in many studies [15–19]. Given the diverse potential thresholds, we selected an expression threshold of 30% to identify patients with high Ki-67 expression consistently. This decision was made to ensure the robustness of our model's performance in the presence of inter-observer variability and differences in the threshold values applied in clinical practice. Our study included all subtypes, including the non-luminal type, to investigate whether DBT could contribute to the

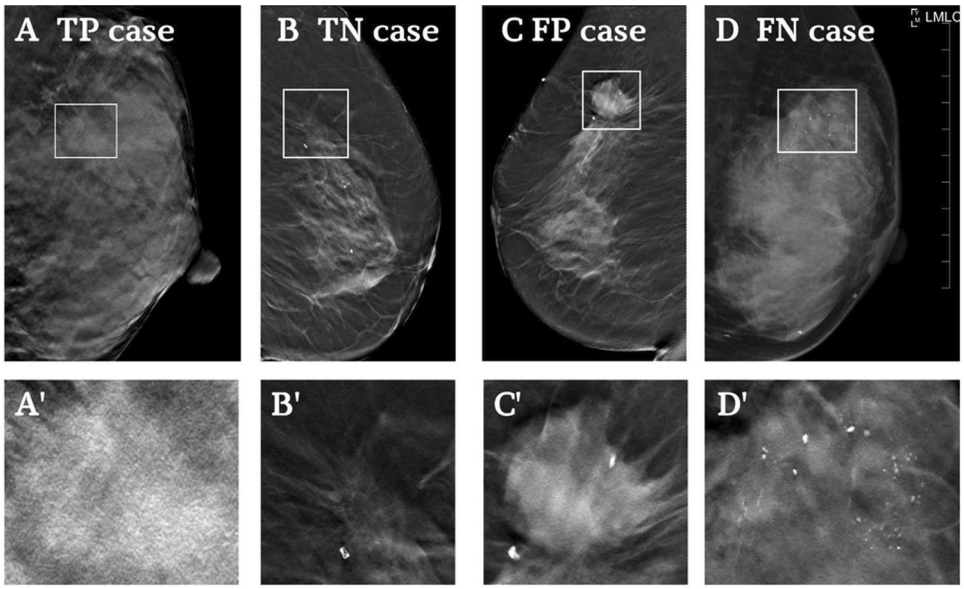

Fig. 3 Representative image from the dataset. **A** Digital breast tomosynthesis (DBT) and cropped image (A') of true positive case (TP). A 46-year-old woman with a high-Ki-67 expression (43%). A spiculated mass was observed during DBT. The entire tumor was included in the study area. Our deep learning (DL) model accurately classified cases with High-Ki67. **B** DBT and cropped image (B') of true negative case (TN). A 75-year-old woman with a low-Ki-67 expression (5%). Distortion was the only observable finding on DBT as no obvious calcification or mass was identified. The DL model accurately classified cases with Low-Ki67. **C** DBT and cropped images (C') of false positive case (FP). A 75-year-old woman with a high-Ki-67 expression (22%). DBT revealed a high-density tumor with distortion on the dorsal side. Our DL model erroneously classified these cases as High-Ki67. **D** DBT and cropped image (D') of a false-positive case (FN). A 50-year-old woman with a high-Ki-67 expression (51%). DBT showing grouped fine pleomorphic and amorphous calcifications spanning 3.0 cm. The cropped ROI did not contain calcifications. Our DL model erroneously classified these cases as Low-Ki67

process of future medical treatment before the results of the histological examination were available. Since Ki-67 expression is determined by histological diagnosis, predicting Ki-67 expression using DBT after subtyping is of little value.

Our study had several limitations. First, it was conducted at a single institution using a single vendor and had a small sample size. This could affect the accuracy of the predictions and limit the generalizability of the findings. In the future, it will be necessary to conduct studies across multiple institutions with larger sample sizes to ensure the robustness of our DL model and its applicability to broader populations. Second, we used cropped images of the lesions in our DL model. For clinical applications, the targeted breast lesions need to be automatically detected. Third, the expression of Ki-67 was obtained in a preoperative biopsy sample. Because of heterogeneity, localized biopsy samples may not represent Ki-67 expression in the entire tumor.

In conclusion, our DL model utilizing DBT has the potential to accurately predict the expression of Ki-67, which can serve as a valuable noninvasive tool for determining the treatment strategy for breast cancer preoperatively.

Authors Contribution Conceptualization: Takuya Ueda and Hiroko Tsunoda; Methodology: Ken Oba, Takuya Ueda, and Hiroko Tsunoda; Investigation: Ken Oba, Toshinori Fukuda, Kazuyo Yagishita, and Hiroko Tsunoda; Formal analysis: Ken Oba; Validation: Maki Adachi, Tomoya Kobayashi, Daiki Shimokawa, and Kengo Takahashi; Data Curation: Ken Oba, Maki Adachi, Daiki Shimokawa, Toshinori Fukuda, Kengo Takahashi, and Hiroko Tsunoda; Software: Maki Adachi, Eichi Takaya, Daiki Shimokawa, and Kengo Takahashi, Resources: Ken Oba, Toshinori Fukuda, Kazuyo Yagishita, and Hiroko Tsunoda; Writing-original draft preparation: Ken Oba, Takuya Ueda, and Hiroko Tsunoda; Writing-review and editing: Maki Adachi, Daiki Shimokawa, Toshinori Fukuda, Kengo Takahashi, and Kazuyo Yagishita; Supervision: Takuya Ueda and Hiroko Tsunoda; Funding acquisition: Takuya Ueda.

Funding This work was supported by JST, CREST JPMJCR15D1, Japan and JSPS KAKENHI 20H03738, Japan.

Data availability The data underlying this research were collected as part of clinical research and have undergone Institutional Review Board (IRB) review, where informed consent was accepted to be waived. This data may be available to future research; however, each new study intending to utilize this data must undergo its own IRB review process to ensure compliance with ethical standards and regulatory requirements.

Declarations

Conflict of interest Takuya Ueda received research grants from JST, CREST JPMJCR15D1, Japan, and JSPS KAKENHI 20H03738, Japan.

References

1. Bray F, Ferlay J, Soerjomataram I, Siegel RL, Torre LA, Jemal A. Global cancer statistics 2018: GLOBOCAN estimates of incidence and mortality worldwide for 36 cancers in 185 countries. CA Cancer J Clin. 2018;68:394–424.
2. Perou CM, Sørlie T, Eisen MB, van de Rijn M, Jeffrey SS, Rees CA, et al. Molecular portraits of human breast tumors. Nature. 2000;406:747–52.
3. Goldhirsch A, Wood WC, Coates AS, Gelber RD, Thürlimann B, Senn H-J. Strategies for subtypes—dealing with the diversity of breast cancer: highlights of the St Gallen International Expert Consensus on the Primary Therapy of Early Breast Cancer 2011. Ann Oncol. 2011;22:1736–47.
4. Lakhani SR, International Agency for Research on Cancer. WHO classification of breast tumors. 2nd ed. Who Classification of Tumors Editorial Board, editor. IARC; 2019.
5. de Azambuja E, Cardoso F, de Castro G, Mano MS, Durbecq V, et al. Ki-67 as prognostic marker in early breast cancer: a meta-analysis of published studies involving 12,155 patients. Br J Cancer. 2007;96:1504–13.
6. Thomssen C, Balic M, Harbeck N, Gnant MS, Gallen V. A brief summary of the consensus discussion on customizing therapies for women with early breast cancer. Breast Care. 2021;2021(16):135–43.
7. Jiang L, Ma T, Moran MS, Kong X, Li X, Haffty BG, et al. Mammographic features are associated with clinicopathological characteristics in invasive breast cancer. Anticancer Res. 2011;31:2327–34.
8. Cheng C, Zhao H, Tian W, Hu C, Zhao H. Predicting the expression level of Ki-67 in breast cancer using multi-modal ultrasound parameters. BMC Med Imaging. 2021;21:150.
9. Fang J, Zhao W, Li Q, Zhang B, Pu C, Wang H. Correlation analysis of conventional ultrasound characteristics and strain elastography with Ki-67 status in breast cancer. Ultrasound Med Biol. 2020;46:2972–8.
10. Surov A, Clauser P, Chang Y-W, Li L, Martincich L, Partridge SC, et al. Can diffusion-weighted imaging predict tumor grade and expression of Ki-67 in breast cancer? A multicenter analysis. Breast Cancer Res. 2018;20:58.
11. Ma W, Ji Y, Qi L, Guo X, Jian X, Liu P. Breast cancer Ki67 expression prediction by DCE-MRI radiomics features. Clin Radiol. 2018;73:909.e1-909.e5.
12. Tagliafico AS, Bignotti B, Rossi F, Matos J, Calabrese M, Valdora F, et al. Breast cancer Ki-67 expression prediction by digital breast tomosynthesis radiomics features. Eur Radiol Exp. 2019;3:36.
13. Truhn D, Schrading S, Haarburger C, Schneider H, Merhof D, Kuhl C. Radiomic versus convolutional neural networks analysis for classification of contrast-enhancing lesions at multiparametric breast MRI. Radiology. 2019;290:290–7.
14. Gao Y, Moy L, Heller SL. Digital breast tomosynthesis: update on technology, evidence, and clinical practice. Radiographics. 2021;41:321–37.
15. Mikami Y, Ueno T, Yoshimura K, Tsuda H, Kurosumi M, Masuda S, et al. Interobserver concordance of Ki67 labeling index in breast cancer: Japan Breast Cancer Research Group Ki67 ring study. Cancer Sci. 2013;104:1539–43.
16. Gudlaugsson E, Skaland I, Janssen EAM, Smaaland R, Shao Z, Malpica A, et al. Comparison of the effect of different techniques for measurement of Ki67 proliferation on reproducibility and prognosis prediction accuracy in breast cancer. Histopathology. 2012;61:1134–44.
17. Jonat W, Arnold N. Is the Ki-67 labelling index ready for clinical use? Ann Oncol. 2011;22:500–2.
18. Polley M-YC, Leung SCY, McShane LM, Gao D, Hugh JC, Mastropasqua MG, et al. An international Ki67 reproducibility study. J Natl Cancer Inst. 2013;105:1897–906.
19. Varga Z, Diebold J, Dommann-Scherrer C, Frick H, Kaup D, Noske A, et al. How reliable is Ki-67 immunohistochemistry in grade 2 breast carcinomas? A QA study of the Swiss Working Group of Breast- and Gynecopathologists. PLoS ONE. 2012;7:e37379.
20. Chollet F. Xception: Deep Learning with Depthwise Separable Convolutions. IEEE Conf Comp Vis Pattern Recogn (CVPR). 2017;2017:1800–7.
21. Deng J, Dong W, Socher R, Li L-J, Li K, Fei-Fei L. ImageNet: A large-scale hierarchical image database. 2009;248–255.
22. Liu L, Jiang H, He P, Chen W, Liu X, Gao J, et al. On the Variance of the Adaptive Learning Rate and Beyond [Internet]. arXiv [cs.LG]. 2019; Available from: http://arxiv.org/abs/1908.03265
23. Jiang T, Jiang W, Chang S, Wang H, Niu S. Intratumoral analysis of digital breast tomosynthesis for predicting the Ki-67 level in breast cancer: A multi-center radiomics study. Medical [Internet]. 2022; Available from: https://aapm.onlinelibrary.wiley.com/doi/abs/https://doi.org/10.1002/mp.15392
24. Zwanenburg A, Leger S, Agolli L, Pilz K, Troost EGC, Richter C, et al. Assessing robustness of radiomic features by image perturbation. Sci Rep. 2019;9:614.
25. Amer HA, Schmitzberger F, Ingold-Heppner B, Kussmaul J, El Tohamy MF, Tantawy HI, et al. Digital breast tomosynthesis versus full-field digital mammography-Which modality provides more accurate prediction of margin status in specimen radiography? Eur J Radiol. 2017;93:258–64.
26. Shimokawa D, Takahashi K, Oba K, Takaya E, Usuzaki T, Kadowaki M, et al. Deep learning model for predicting the presence of stromal invasion of breast cancer on digital breast tomosynthesis. Radiol Phys Technol. 2023. https://doi.org/10.1007/s12194-023-00731-4.
27. Bustreo S, Osella-Abate S, Cassoni P, Donadio M, Airoldi M, Pedani F, et al. Optimal Ki67 cut-off for luminal breast cancer prognostic evaluation: a large case series study with a long-term follow-up. Breast Cancer Res Treat. 2016;157:363–71.
28. Johnston SRD, Harbeck N, Hegg R, Toi M, Martin M, Shao ZM, et al. Abemaciclib Combined With Endocrine Therapy for the Adjuvant Treatment of HR+, HER2-, Node-Positive, High-Risk, Early Breast Cancer (monarchE). J Clin Oncol. 2020;38:3987–98.
29. Honma N, Yoshida M, Kinowaki K, Horii R, Katsurada Y, Murata Y, et al. (2023) The Japanese breast cancer society clinical practice guidelines for pathological diagnosis of breast cancer, 2022 edition. Breast Cancer, doi: https://doi.org/10.1007/s12282-023-01518-6.